Monte Carlo simulations of spatial correlations of charges on a random lattice: positional versus thermal disorder

Monte Carlo simulations of spatial correlations of charges on a random lattice: positional versus thermal disorder

P Sobkowicz, Z Wilamowski and J Kossut

Institute of Physics, Polish Academy of Sciences, Al. Lotników 32/46, 02-668 Warsaw, Poland

Abstract. Monte Carlo simulations of a system of point charges occupying a fraction of a random array of sites in two and three dimensions are reported. We focus on the Coulomb-interaction-driven ordering phenomena in the system. The model corresponds directly to the details of physics of charges of partially filled resonant impurities in a semiconductor, but qualitative results are of wider significance. Spatial correlations of charges, due to long-range repulsive interactions between them, are studied as a function of temperature by means of pair correlation functions and one-particle density of states. The presence of inherent disorder of the allowed positions of the impurity charges is found to influence the ordering process, leading to a saturation of correlation range at low temperatures. Such behaviour is not observed in a pseudo-liquid model also studied for the sake of comparison. Within the latter model the charges are assumed to have the same densities, and interactions to have the same strength, but instead of being restricted to a random array of sites the charges are allowed to take any position. Comparison of the two models allows us to introduce a phenomenological effective temperature, which includes the effects of the built-in disorder on the same footing as the thermal disorder. The formation of the Coulomb gap in the density of states is discussed and its relation to the Madelung gap in crystalline materials pointed out.

1. Introduction

This paper presents results of Monte Carlo (MC) studies of spatial ordering phenomena in a system of point charges occupying a fraction of a random array of fixed sites. A repulsive interaction between the charges leads to correlations between their positions. Namely, the charges tend to arrange themselves as far away from each other as possible, within the limits imposed by the availability of sites. The degree of ordering due to the interaction depends on many properties of the system: temperature, charge density, strength of the interaction, screening length, etc. We discuss the influence of the built-in disorder on correlations in the system. The problem of a co-existence of an inherent disorder and the correlations stemming from Coulombic interactions is of importance not only in materials with charged impurities (upon which the present paper focuses its attention) but also in a wider class of semiconducting systems, e.g. those displaying integer and fractional quantum Hall effect. Such an influence has been previously studied and discussed in the case of charge density waves on a random alloy and flux lines in high-temperature superconductors [1].

The fact that positions of the charges are restricted to a randomly distributed and fixed set of sites and the absence of kinetic energy distinguishes our study from previous studies of ordering in electron gas [2–4], liquids and colloidal suspensions [5–15]. Our system describes an example of the interplay between thermal and built-in disorder, namely spatial correlations of charges in an incompletely filled system of impurities resonant with the

conduction band in semiconductors, in both two- and three-dimensional geometries. The electrons that occupy the impurities (donors, to be more specific) can hop from one site to the other and, in such a fashion, lower the energy of the entire system. The qualitative results, however, should have a wider significance. The correlations in the described system have been studied previously mainly in the zero-temperature regime, and for a three-dimensional situation [16–19], using analytical models and the zero-temperature MC formalism. Results describing the temperature dependence of the correlations have been rather limited [20,21].

The three- and two-dimensional systems studied here correspond, in our example, to bulk semiconductors and planar- (or δ-) doped semiconducting structures, respectively. We describe of the temperature dependence of the pair distribution function, $g(R)$, density of states (DOS); we also discuss the formation of the so-called Coulomb gap [2] and its close relation to the Madelung gap in crystalline structures. It is possible to trace the influence of the randomness of the distribution of available sites—stemming from the fact that the impurities replace atoms of the host semiconductor lattice in a random fashion (we call this type of randomness in the system 'the positional disorder')—on the ordering of charges located on them and to compare it with the influence of thermal fluctuations. To single out the effects due to the positional disorder we compare our system with its 'pseudo-liquid' counterpart in which the charges interacting by means of the same potential and having *no* kinetic energy are allowed to assume arbitrary positions. The pseudo-liquid model may also be looked upon as a limiting case of the random impurity model, with the density of available sites diverging to infinity with the density of charges kept constant. By comparing the two models we were able to understand the limitations imposed on the ordering process by the positional disorder and introduce a simple phenomenological description of a joint effect of both the positional and thermal disorder.

2. The model and method of calculation

In this work we consider a random array of fixed sites (either in 3D space or on a 2D plane). We assume that some of these sites may be electrically charged. The ratio of the charged-sites density to the total-site density, which will be called the occupation fraction, f, plays a crucial role in the studied phenomena. The total charge neutrality is preserved by the presence of a continuous charge of opposite sign, corresponding to a conduction-band electron gas in the host semiconductor or a 2D electron layer near the δ-doping plane. This cloud of conduction electrons is uniformly spread out and does not introduce any additional disorder into the system. This choice distinguishes our work from previous studies of correlations in compensated semiconductors, where the charge neutrality is provided by doping with both donors and acceptors [2,3,22,23]. In such a case, the neutralizing charge is localized on randomly distributed acceptors, thus being a source of another randomness in the system. In our case, in addition to providing the charge neutrality, the electrons screen the Coulomb interaction between the impurity charges. The exact description of the screening is quite difficult, particularly in the case of quasi-2D electron layers [24]. We have used instead a Yukawa approximation both in the 3D and 2D situation:

$$V(r) = \frac{e^2}{\varepsilon_0 \varepsilon} \frac{1}{r} \exp\left(-\frac{r}{\lambda}\right) \tag{1}$$

with ε being the dielectric constant of the semiconductor host and λ representing the screening radius, which in the majority of cases presented in this paper will be assumed to

be a constant quantity. Numerical values of these two parameters employed in this paper were intended to render the real situation in HgSe doped with Fe resonant donors (3D case) or in δ-doped GaAs: two systems where experimental data concerning spatial correlations of the impurity charges are available. Namely, we have used $\varepsilon = 12.4$ in 2D simulations and $\varepsilon = 20$. The relative insensitivity of the results on the actual value of the screening length λ was already noted in [25]. We checked in our study that this, admittedly somewhat surprising fact, does occur. Therefore, we decided to omit in the majority of this work any dependence of λ on, for example, the density of conduction electrons, i.e. on the number of charged impurity sites. The simple form of (1) allows us to focus attention on the physics of correlations, and not on the complications due to the exact form of the potential. Furthermore, the use of a simple form of screening also allows comparisons with results obtained for Yukawa liquids and colloidal suspensions [10–14]. We have used numerical values of the screening length λ close to those given by Thomas–Fermi theory for the appropriate materials (for the 2D systems we have used, as an approximation, an average spatial density of electrons in a quasi-2D layer). Unless otherwise indicated, the value used for 2D systems is $\lambda^{2D} = 50\text{Å}$, and for the 3D systems $\lambda^{3D} = 65\text{Å}$.

We have studied the ordering phenomena using standard Monte Carlo techniques [26, 27]. We used models with up to 2000 sites, with a cubic or square geometry and periodic boundary conditions. We have used the minimal-image convention, in which a given charge interacts only with nearest copies of other charges. This is a natural method for systems where the screening length is much smaller than the size of the unit cell used in simulations. We have added the contribution of averaged interactions with charges outside the directly considered volume. This additional term changed the absolute values of the site energies, but did not influence the ordering.

The pseudo-liquid model consisted of charged centres which during the simulations were allowed to change positions arbitrarily, starting from an initial random distribution. The final point of a jump has been chosen randomly from within a sphere around the starting point. The radius of the sphere has been chosen approximately equal to the mean separation of charges. The density of charges and the interaction between them remained the same as in the random impurity model. In the ideal case, at low temperatures the pseudo-liquid system should crystallize and form a lattice. In the 2D case the lattice is triangular, whereas in the 3D case it is either BCC or FCC, depending on the ratio of the distance between charges and screening length [10]. In practice, due to relatively fast quench rates imposed by computational resources, only the transition to the glassy state has been observed, as indicated, for example, by splitting of the second neighbour peak in the pair correlation function $g(R)$ (see figure 4). It should be noted here that the results of the pseudo-liquid model are far from exhaustive, and are used only as a reference point to determine the influence of a random distribution of the available positions in the impurity model on ordering phenomena.

3. Results

We present various results of the Monte Carlo simulations which offer different measures of the ordering phenomena in the system. For example, we show results concerning the pair correlation function, one-particle density of impurity states and its second moment. All the presented quantities indicate that below a certain temperature (dependent on model parameters like screening length and occupation fraction) correlations in the random impurity

model become frozen, with a certain amount of residual disorder. The comparative pseudo-liquid model shows no such behaviour until much lower temperatures, and the degree of ordering is much higher there.

All the results for the 2D case are presented for a sheet doping density of 10^{13} cm^{-2} (typical for the δ-doping layers). In the 3D case the assumed doping density is 1.5×10^{19} cm^{-3}. The later value is chosen to correspond to experimental situation where the effects of correlations are found to be the strongest in HgSe doped with Fe [28, 29]. Moreover, despite the difference in dimensionality, the above choice of densities leads to similar length scales in 2D and 3D systems with the same occupation fractions.

3.1. Pair correlation function

Figure 1 presents examples of the pair correlation function $g(R)$ for 2D and 3D systems at an occupation fraction $f = 0.3$. The general features of the pair correlation function may be described as follows.
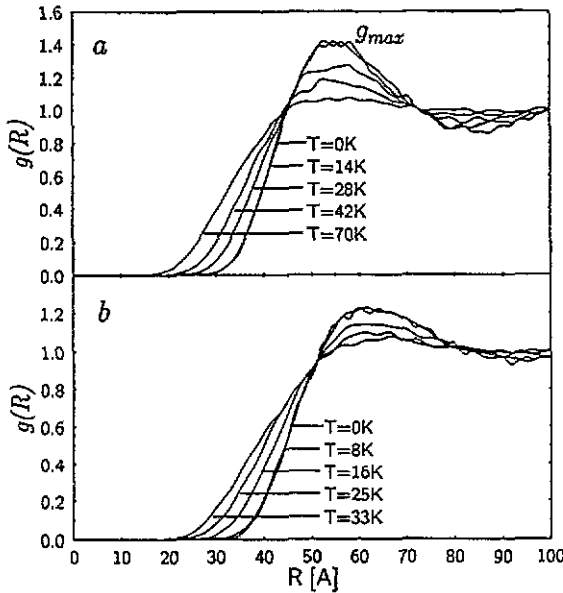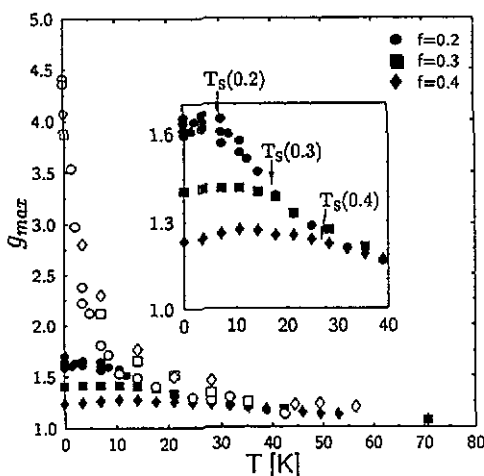

Figure 1. Examples of the pair correlation functions for an occupation fraction $f = 0.3$ and various temperatures. (*a*) Two-dimensional system; (*b*) three-dimensional system.

For high occupation fractions or high temperatures $g(R)$ resembles roughly a step-like function: $g(R) = 0$ for $R < R_c$, $g(R) = 1$ for $R \geqslant R_c$, used in the analytical short-range correlation model [16, 19]. This behaviour is due to strong repulsion between charges located on close pairs (see, for example, [6]). High temperatures, or a small number of available neutral sites, do not allow ordering beyond the nearest neighbourhood.

At low temperatures and low occupation fractions f, a significant deviation from the short-range model appears, in the form of well resolved maxima and minima in $g(R)$, corresponding to consecutive neighbour shells. The presence of medium- and long-range order in a system with a soft (i.e. not hard core) and purely repulsive potential has been widely studied before (see, for example, [13], and references therein), and the fluid–solid transition for repulsive forces is known as the Kirkwood–Alder transition.

For a given f, the structure in $g(R)$ at first increases with decreasing temperature, which signifies ordering of the system, and then saturates below a certain temperature $T_S(f)$, depending on the occupation fraction value and screening constant λ. Figure 2 presents

Figure 2. Temperature dependence of the height of the first neighbour peak g_{max} in the pair correlation function for a 2D system. Filled symbols represent results of MC simulations for the random impurity model, empty symbols are for the pseudo-liquid model. Multiple points for given temperatures that correspond to runs of the MC simulation differing in cooling rate and sample size. The inset shows details of g_{max} for a random impurity system in the low-temperature limit, with saturation temperatures marked by arrows.
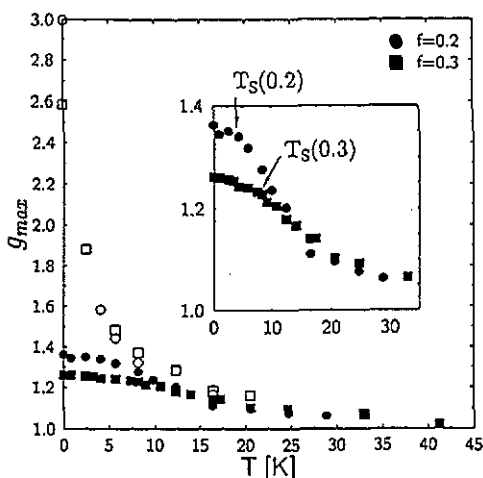
Figure 3. Temperature dependence of the height of the first neighbour peak g_{max} in the pair correlation function for a 3D system. Filled symbols represent results of MC simulations for the random impurity model, empty symbols are for the pseudo-liquid model. The inset shows details of g_{max} for a random impurity system in the low-temperature limit, with saturation temperatures marked by arrows.

the temperature dependence of the first neighbour peak of $g(R)$, g_{max}, as a function of the temperature for three occupation fractions $f = 0.2, 0.3, 0.4$ in the 2D case. A similar result for the 3D case is shown in figure 3. The saturation temperature seems to be better defined in the case of 2D systems, with a more rounded shape for 3D systems. The saturation values of g_{max} are higher for lower occupation fractions. At the same time, the saturation itself takes place at lower temperatures $T_S(f)$. This reflects the fact that for lower occupation fractions more neutral sites are available, and the system is able to achieve better ordering.

The pseudo-liquid model also shows an enhancement of the structure in $g(R)$ with a decreasing temperature. For temperatures above $T_S(f)$ the random impurity and the pseudo-liquid model give similar results. Below $T_S(f)$, on the other hand, there is a large difference between the results given by the two models. Whereas the ordering process in the random impurity model seems to come to a stop, in the pseudo-liquid model it continues until very low temperatures.

The difference is particularly clear when one compares the corresponding pair correlation functions and actual charge distributions for the random impurity and pseudo-liquid models at $T \approx 0$. Figure 4 presents such a comparison for the 2D system, where visualization is easier. In the random impurity model the only ordering visible is a correlation of spatial separation between charges (figure 4(c)). On the other hand, in the pseudo-liquid model one can clearly define regions with orientational order (figure 4(d)). This results in a much more pronounced structure in $g(R)$ for the pseudo-liquid model (figure 4(b)), with splitting of the second neighbour peak, characteristic for long-range ordering.

The values of the saturation temperatures depend on the assumed screening length,
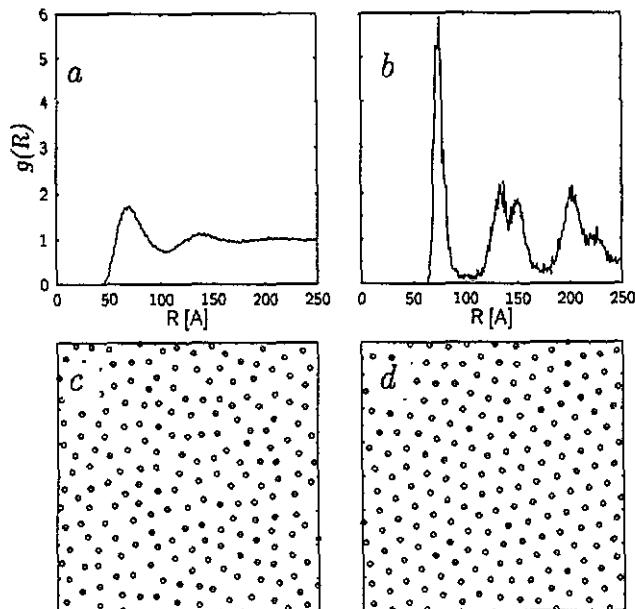
Figure 4. Comparison of pair correlation functions for the random impurity and pseudo-liquid models of the 2D system at occupation fraction $f = 0.2$, and $T \approx 0$. (*a*) $g(R)$ for the random impurity model. (*b*) $g(R)$ for the pseudo-liquid model. (*c*) Example of spatial charge distribution for the random impurity model inside a 1000 Å × 1000 Å square. (Most of charged impurities contained in the simulated system are not shown in the figure). (*d*) Example of spatial charge distribution for the pseudo-liquid model inside a 1000 Å × 1000 Å square. (Most of the charged impurities contained in the simulated system are not shown in the figure.) Long-range orientational ordering, clearly visible in the pseudo-liquid model (where the charges may assume arbitrary positions during the simulations) is absent in the random impurity model, in which charges are restricted to a randomly distributed set of sites. The splitting of the second peak in the $g(R)$ for the pseudo-liquid model is one of the characteristic features of glass formation [14].

diminishing with decreasing λ. However, in the random impurity system, at $T = 0$, the shape of $g(R)$ and the g_{max} value do not change over a wide range of λ values, from λ much smaller than the mean separation between the charges (see figure 5). Only for very small values of λ have we observed a change in $g(R)$. This deviation requires further study, the results of which will be published elsewhere.

The importance of the pair correlation function results from the fact that $g(R)$ is directly related to the structure factor $S(q)$, determining the scattering rate from ionized impurity scattering. Enhancement of correlations with decreasing temperature leads to an increase of electron mobility. Thus, the saturation of the ordering, expressed by freezing of $g(R)$ below $T_S(f)$ leads to a halt of the increase of the mobility with decreasing T. Possibly this fact is related to a saturation of mobility in HgSe:Fe at low temperatures observed by Lenard and co-workers [30, 31] and Pool and co-workers [28, 29].

3.2. Density of states

The pair correlation function gives a rather limited view of the ordering phenomena—there exist higher-order correlation functions which contain more information. Still another method of quantification of the amount of disorder in a system is through a study of
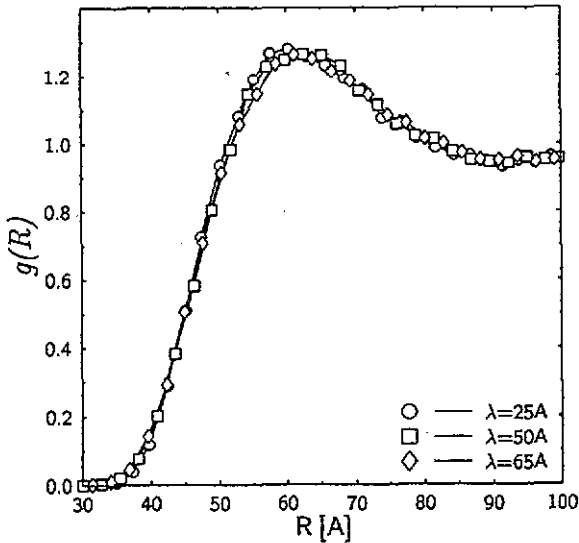
Figure 5. Pair correlation function for the 3D system, $T = 0$ and $f = 0.3$ for different values of the screening length λ. Even for λ much lower than the separation between the nearest neighbours (given by the position of peak in $g(R)$), the pair correlation function remains unchanged.

the energy distribution, given by the density of states (DOS). This quantity, frequently used in the physics of semiconductors, is seldom used in studies of liquids and colloids, although it offers interesting insights into many phenomena. The single-particle DOS allows a description of the mean value and fluctuations of the energy of particles.

Computer simulations offer a simple and direct way of describing the energy distribution in the simulated system. One can simply record values of the electrostatic potential at lattice sites, due to all charges except the one located at the given site. In the case of a charged site this corresponds simply to the electrostatic energy of the charge. In the case of a neutral site, this gives the energy of a test charge located on the site. In this sense one can speak of energies of charged and empty sites. The above approach can be extended to the pseudo-liquid model, only the energy distribution of neutral sites is replaced by continuum of energies of test charges at all unoccupied points in space. In our work we will study the dispersion of site energies and relation of energies of charged and neutral sites. A typical example of the energy distribution of various species of impurity site is presented in figure 6, which shows all important aspects of the density of states of the systems under study here.

3.2.1. Broadening of the density of states. As can be seen in figure 6 the distribution of energies of charged sites has a roughly Gaussian shape, becoming asymmetrical with an increasing temperature. Further examples of DOS are presented in figures 7 and 8. In this section we shall concentrate on the second moment of the energy distribution of charged sites, $\sigma^2(f, T) = (E - \overline{E(f, T)})^2$, where the bar denotes averaging with respect to energy. Figures 9 and 10 present the behaviour of $\sigma^2(f, T)$ for various occupation fractions and temperatures, for the 2D and 3D case, respectively. Results for the random impurity model (filled symbols) show a similar type of behaviour as the pair correlation function: with decreasing temperature, σ^2 at first decreases and then saturates below temperatures approximately equal to the values of $T_S(f)$ obtained from the study of pair correlation functions. One can also observe that here, as in the analysis of $g_{max}(T)$, the saturation temperatures are easier to define in the 2D systems. In the pseudo-liquid model there is no saturation, except at extremely low temperatures when, in some cases, a transition to the glass phase has been observed. Instead, the dispersion σ^2 decreases approximately linearly
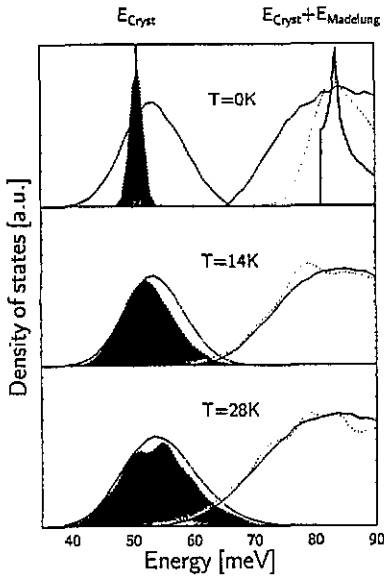
Figure 6. Comparison of density of states for a 2D random impurity and pseudo-liquid systems. Light gray area: DOS of charged sites in the random impurity system. Dark gray area: DOS of charged sites for the pseudo-liquid model. Full curve: DOS of neutral sites in the random impurity model; dotted curve: DOS for the continuum of neutral sites for the pseudo-liquid model. The thick full curve represents the perfect crystalline arrangement of charges. The DOS of neutral sites for the pseudo-liquid model and crystal (which are not properly normalized) are scaled to become comparable with the random impurity model. E_{cryst} is the energy of lattice sites in a crystalline array with the same charge density, $E_{Madelung}$ is the value of the Madelung gap in the crystal. One can note that at low temperatures the shape of the DOS for the random impurity model does not change, whereas in the pseudo-liquid model a finite region of energies with DOS $= 0$ develops. At higher temperatures both models give similar results.
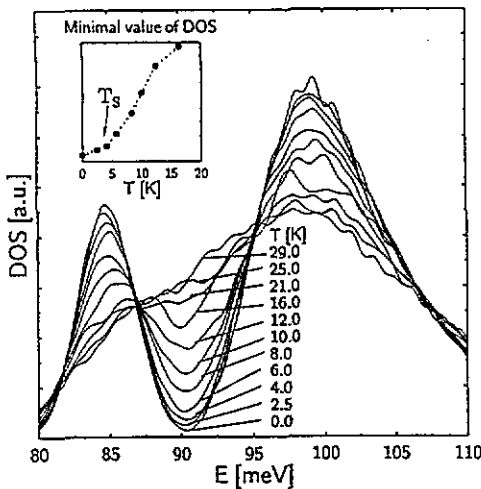

Figure 7. Total density of states (summed DOS of charged and neutral sites) for the 3D random impurity model. The small but non-zero value at $T \approx 0$ is due to averaging between different realizations of the system. The inset shows the dependence of the minimal value of the DOS at the centre of the Coulomb gap as a function of temperature. Occupation fraction $f = 0.2$.
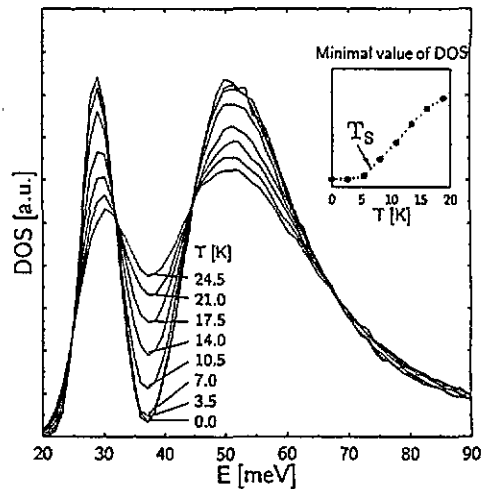

Figure 8. The same as figure 7, but for a 2D random impurity model with $f = 0.2$.

with decreasing temperature (open symbols in figures 9 and 10).

To analyse the temperature dependence of σ^2 in a more quantitative way we have fitted a simple empirical formula to the results of the random impurity model:

$$\sigma^2(f, T) = \sigma_0^2(f)\sqrt{T^2 + T_0^2(f)} \qquad (2)$$

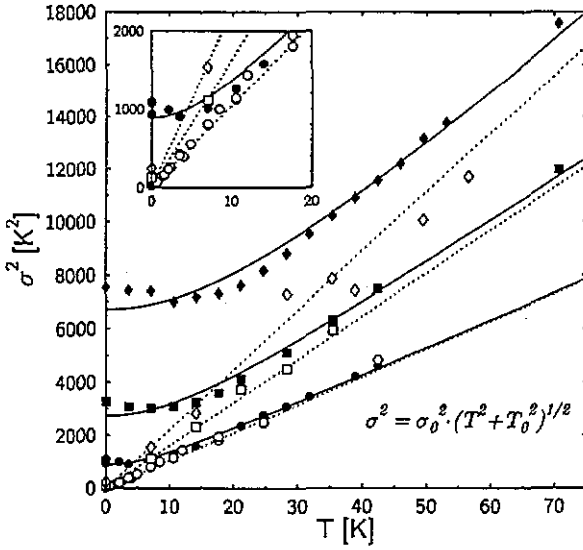interpreting $T_0(f)$ as a thermal measure of the effects due to positional disorder. Taking

Figure 9. Second moment of the energy distribution for 2D systems of various occupation fractions as a function of temperature. Diamonds: $f = 0.4$; squares: $f = 0.3$; circles: $f = 0.2$. Filled symbols: random impurity model; open symbols: equivalent pseudo-liquid model. The inset shows the details at low temperatures. The full curves are the results of the fit $\sigma^2 = \sigma_0^2 \sqrt{T^2 + T_0^2}$ to the random impurity MC simulations results. Dotted curves, coinciding very well the results of the pseudo-liquid model, correspond to the linear function $\sigma^2 = \sigma_0^2 T$ with the same σ_0 as in the corresponding random impurity models. The inset shows the details in the low-temperature region.
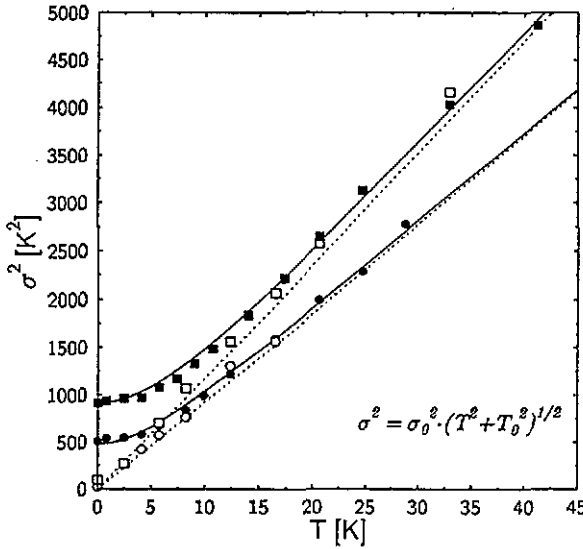
$$\sigma^2 = \sigma_0^2 \cdot (T^2 + T_0^2)^{1/2}$$

$$\sigma^2 = \sigma_0^2 \cdot (T^2 + T_0^2)^{1/2}$$

Figure 10. The same as in figure 9, but for 3D systems. Squares: $f = 0.3$; circles: $f = 0.2$.

into account numerical errors, the above formula describes remarkably well the results of MC simulations in both 2D and 3D cases (the full curves in figures 9 and 10). Comparing the values of $T_0(f)$ with the corresponding approximate saturation temperatures $T_S(f)$ obtained from the study of g_{max} show that both quantities are indeed closely related: see table 1.

Table 1. Comparison of $T_0(f)$ and $T_S(f)$.

	2D case			3D case	
f	0.2	0.3	0.4	0.2	0.3
$T_S(f)$	7 ± 2	16 ± 3	27 ± 5	4 ± 2	8 ± 3
$T_0(f)$	8.6	17.0	30.2	5.2	7.8

The above interpretation of $T_0(f)$ is in accord with the analysis of the results found for the pseudo-liquid system: using the values of $\sigma_0^2(f)$ derived from the random impurity model, and putting $T_0(f) = 0$ we have obtained simple linear functions $\sigma^2(f, T) = \sigma_0^2(f)T$ (the broken curves in figures 9 and 10). It may be seen that this simple approach provides a good description of the properties of the pseudo-liquid system in all cases studied (open symbols in figures 9 and 10). This allows us to describe positional disorder using thermal measures, for example, introducing an effective temperature $T^* = \sqrt{T^2 + T_0(f)^2}$. In other words, T_0 itself is a measure of the positional disorder alone.

The possibility of expressing at least some of the effects of positional disorder in a random impurity model is especially important in the light of recent attempts to describe temperature and doping concentration dependence of mobility in HgSe doped with iron using a formalism from liquid state theory [32, 33]. As indicated by our work, direct application of liquid-like models seems to be an oversimplification, especially at low temperatures. However, using the effective temperature T^* could lead to a more realistic description of the system.

Let us note here that the positional disorder in the sense used in this work is completely different from the 'internal disorder', i.e. the scatter of the impurity site energies introduced, for instance, in [2]. In our models the energies of the impurities without interactions are all the same.

3.2.2. A gap in the density of states. A comparison of the distribution of potential energies of charged and neutral sites such as presented in figure 6 reveals another striking feature due to interaction between charges: the so-called Coulomb gap [2–4, 22, 23, 34]. The name describes a pronounced drop in the total one-particle DOS (i.e. the summed DOS of neutral and charged sites) found at low temperatures, separating the energies of charged and neutral sites (figures 6–8). The Coulomb gap has been initially found in numerical studies of highly doped semiconductors with internal disorder [2, 22, 23]. Recently, Efros [4] studied the formation and temperature dependence of the Coulomb gap in a system of point charges without external disorder (corresponding to our pseudo-liquid model with Coulomb instead of Yukawa interactions).

In this work we propose a unifying picture describing the behaviour of the DOS in a system of point charges, valid for a whole range of systems, starting from perfect crystals and ending with a totally random distribution of charges. We argue that the formation of a gap in the density of states, separating energies of charged and neutral sites, is due to the presence of spatial ordering imposed by electrostatic repulsion of the charges and that it appears even for relatively short-range potentials (with the screening length of the order of the inter-impurity separations.

Let us consider first a perfect lattice of charges. All of them have the same energy, E_{cryst}, thus the DOS of the charged sites is a Dirac delta function. On the other hand, a test charge located at any point except for the lattice sites has a higher potential energy. In fact, there is a finite difference between the energy of lattice (charged) sites and the lowest energy of non-lattice (neutral) sites. This difference may be named the Madelung gap, $E_{Madelung}$ (see figure 6(a)).

An increase of the temperature broadens the energy distribution of both charged and neutral sites. The broadening is due to the movement of the position of the charges around the lattice sites and to the formation of defects. The uppermost panel in figure 6 presents the DOS of a supercooled 2D liquid (the dark gray area represents charged sites, the broken curve the continuum of neutral sites). Although the energy distributions are broadened, there is still a well defined region of energies where the DOS is equal to zero. For comparison, the

DOS of the random impurity system is also shown.

A further increase of temperature gradually closes the finite gap in the density of states for the pseudo-liquid model, and leads to a situation such as is presented in the middle panel of figure 6. The DOS of the pseudo-liquid and the random impurity models become very similar. The exact shape of the DOS depends not only on the dimensionality of the system, as previously suggested, but also to the amount of disorder present. The process of gap-filling continues with increasing temperature until finally, at sufficiently high temperatures, the gap in the DOS disappears. Figures 7 and 8 present the detailed temperature dependence of the DOS shape for a 2D and 3D random impurity system with $f = 0.3$. The insets show that the temperature dependence of the minimal value of the DOS also shows a change in behaviour at temperatures close to $T_S(f)$ or $T_0(f)$. A small but finite value of the DOS at the minimum for $T = 0$ is a result of averaging between various numerical realizations of the systems, smearing the Fermi energy. For a system with 'positional disorder', having a filling fraction $f \approx 0.5$ and at very low temperature, we expect σ^2 to be of the order of the Coulomb gap width since both quantities scale approximately with the interaction energy characteristic for the first coordination distance. On the other hand, for f approaching zero the dispersion σ^2 drops while Coulomb gap becomes more pronounced.

We think that it is important to point out the close connection between the existence and shape of the Coulomb gap in the density of states with the degree of spatial ordering in the system. The ordering, in turn, is due to the repulsion between charges. The presence of the built-in disorder, as in the random impurity system, may stop the transition from the traditional Coulomb to Madelung gap at a certain point. The resulting shape of the DOS at $T \approx 0$ thus depends, for example, on the ratio of the number of charges to the number of available sites.

4. Conclusions

We have studied a system of charges located on a random array of sites and interacting through a Yukawa potential. In this system the spatial ordering of charges is blocked at low temperatures by the presence of built-in underlying positional disorder. The ordering process is described with the help of several physical quantities: pair correlation functions, fluctuations of individual site energy, Coulomb gap formation in the density of states. All studied examples, both two- and three-dimensional, show saturation of correlations below a certain temperature. The value of the saturation temperature depends on the occupation fraction, f, defined as the ratio of the charged-sites density to the total-site density, screening length and dimensionality, although not very sensitively on the latter two. Lack of sensitivity to the screening length (determined mainly by the conduction electron density) can be understood, remembering that for a spatially correlated impurity system the important contribution to effective screening of the impurity potentials comes from self-screening within the impurity system. A comparison of the results of the random impurity model with a pseudo-liquid model (corresponding to the limiting case of $f \to 0$ with constant charge density and screening length) allows us to emphasize the role of an interplay between thermal disorder and positional disorder due to initial random distribution of available sites. It has been possible to introduce an 'empirical' temperature T_0, describing the effects of positional disorder. T_0 roughly corresponds to temperatures below which there is no further ordering with decreasing temperature.

Acknowledgments

References

[1]   Dai H and Lieber C M 1992 *Phys. Rev. Lett.* **69** 1576
[2]   Efros A L and Shklovskii B I 1985 *Electron–Electron Interactions in Disordered Systems* ed. A L Efros and M Pollak (Amsterdam: Elsevier) p 409
[3]   Davies J H, Lee P A and Rice T M 1984 *Phys. Rev.* B **29** (1984) 4260
[4]   Efros A L 1992 *Phys. Rev. Lett.* **68** 2208
[5]   Hansen J-P and Weis J J 1977 *Mol. Phys.* **33** 1379
[6]   Hansen J-P and Hayter J B 1982 *Mol. Phys.* **46** 651
[7]   Yonezawa F 1991 *Solid State Physics* **45** ed. D Turnbull and H Ehrenreich (New York: Academic) p 179
[8]   Abraham F F 1982 *Melting, Localization and Chaos* ed. R K Kalia and P Vashishta (Amsterdam: Elsevier) p 75
[9]   Vashishta P and Kalia R K 1982 *Melting, Localization and Chaos* ed. R K Kalia and P Vashishta (Amsterdam: Elsevier) p 43
[10]   Robbins M O, Kremer K and Grest G S 1988 *J. Chem. Phys.* **88** 3286
[11]   van Megen W and Snook I 1977 *J. Chem. Phys.* **66** 813
[12]   Pistoor N and Kremer K 1989 *Dynamics of Disordered Materials* ed. D Richter, A J Dianoux, W Petry and J Texeira (Berlin: Springer) p 91
[13]   Sood A K 1991 *Solid State Physics* **45** ed. D Turnbull and H Ehrenreich (New York: Academic) p 1
[14]   Kesavamoorthy R, Sood A K, Tata B V R and Arora A K 1988 *J. Phys. C: Solid State Phys.* **21** 4737
[15]   Murray C A, Sprenger W O and Wenk R A 1990 *Phys. Rev.* **42** 688
[16]   Kossut J, Wilamowski Z, Dietl T and Światek K 1990 *The Physics of Semiconductors* ed. E M Anastassakis and J D Joannopoulos (Singapore: World Scientific) p 613
[17]   Kossut J, Wilamowski Z, Dietl T and Światek K 1991 *Acta Phys. Polon.* A **79** 49
[18]   Kossut J, Wilamowski Z, Dietl T and Światek K 1990 *Semicond. Sci. Technol.* **5** S260
[19]   Wilamowski Z, Światek K, Dietl T and Kossut J 1990 *Solid State Comm.* **73** 833
[20]   van der Wel P J, Anders M J, Giling L J and Kossut J 1993 *Semicond. Sci. Technol.* to be published
[21]   MogilyanskiiA A and Raikh M É 1989 *Sov. Phys.–JETP* **68** 1081
[22]   Baranovskii S D, Efros A L, Gelmont B L and Shklovskii B I 1979 *J. Phys. C: Solid State Phys.* **12** 1023
[23]   Bello M S, Levin E I, Shklovskii B I and Efros A L 1981 *Zh. Eksp. Teor. Fiz.* **80** 1596 (Engl. transl. 1981 *Sov. Phys.–JETP* **53** 822)
[24]   Bastard G 1988 *Wave Mechanics Applied to Semiconductor Heterostructures* (Les Ulis: Editions de Physique)
[25]   Światek K, Dietl T, Wilamowski Z and Kossut J 1988 *Proc. 19th Int. Conf. on Phys. of Semiconductors, Warsaw 1988* ed. W Zawadzki (Warsaw: Institute of Physics) p 1571
[26]   Metropolis N, Rosenbluth A W, Rosenbluth M N, Teller A H and Teller E 1953 *J. Chem. Phys.* **21** 1087
[27]   Binder K (ed) 1986 *Monte Carlo Methods in Statistical Physics* (Berlin: Springer)
[28]   Pool F S, Kossut J, Debska U and Reifenberger R 1987 *Phys. Rev.* B **35** 3900
[29]   Pool F S, Reifenberger R and Miller M M 1990 *Phys. Rev.* B **41** 1625
[30]   Lenard A, Dietl T, Sawicki M, Dybko K, Dobrowolski W, Skośkiewicz T, Plesiewicz W and Mycielski A 1989 *Acta Phys. Polon.* A **75** 249
[31]   Lenard A, Dietl T, Sawicki M, Dobrowolski W, Dybko K, Skośkiewicz T, Plesiewicz W, Miotkowska S, Witek A and Mycielski A 1990 *J. Low Temp. Phys.* **80** 15
[32]   Tsidlikovskii I M, Kuleev I G and Lyapilin I I 1993 to be published
[33]   Kuleev I G, Lyapilin I I and Tsidlikovskii I M 1993 to be published
[34]   Shklovskii B I and Efros A L 1984 *Electronic Properties of Doped Semiconductors (Springer Series in Solid-State Sciences 45)* (Berlin: Springer)